

AD-A158 396

DERIVATION OF THE OPTICAL CONSTANTS OF ANISOTROPIC MATERIALS

James R. Aronson, Alfred G. Emslie
Emmett M. Smith and Peter F. Strong

July 31, 1985

U.S. ARMY RESEARCH OFFICE

DAAG-29-82-C-0017

ARTHUR D. LITTLE, INC.
Cambridge, Mass.

APPROVED FOR PUBLIC RELEASE;
DISTRIBUTION UNLIMITED

DTIC FILE COPY

②

DTIC
ELECTE
AUG 28 1985
S
D

REPORT DOCUMENTATION PAGE		READ INSTRUCTIONS BEFORE COMPLETING FORM
1. REPORT NUMBER <i>ARO 18649.5-CH</i>	2. GOVT ACCESSION NO. <i>AD-4158 396</i>	3. RECIPIENT'S CATALOG NUMBER
4. TITLE (and Subtitle) DERIVATION OF THE OPTICAL CONSTANTS OF ANISOTROPIC MATERIALS		5. TYPE OF REPORT & PERIOD COVERED FINAL - 7/82 - 7/85
7. AUTHOR(s) James R. Aronson, Alfred G. Emslie, Emmett M. Smith and Peter F. Strong		6. PERFORMING ORG. REPORT NUMBER
9. PERFORMING ORGANIZATION NAME AND ADDRESS Arthur D. Little, Inc. Acorn Park Cambridge, Mass. 02140		8. CONTRACT OR GRANT NUMBER(s) DAAG-29-82-C-0017
11. CONTROLLING OFFICE NAME AND ADDRESS U. S. Army Research Office Post Office Box 12211 Research Triangle Park, NC 27709		10. PROGRAM ELEMENT, PROJECT, TASK AREA & WORK UNIT NUMBERS
14. MONITORING AGENCY NAME & ADDRESS (if different from Controlling Office)		12. REPORT DATE 7/31/85
		13. NUMBER OF PAGES 32
		15. SECURITY CLASS. (of this report) Unclassified
		15a. DECLASSIFICATION/DOWNGRADING SCHEDULE
16. DISTRIBUTION STATEMENT (of this Report) Approved for public release; distribution unlimited		
17. DISTRIBUTION STATEMENT (of the abstract entered in Block 20, if different from Report) NA		
18. SUPPLEMENTARY NOTES The view, opinions, and/or findings contained in this report are those of the author(s) and should not be construed as an official department of the Army position, policy, or decision unless so designated by other documentation.		
19. KEY WORDS (Continue on reverse side if necessary and identify by block number) Optical Constants; Triclinic Crystals; Monoclinic Crystals; Complex Dielectric Tensor; Anisotropic crystals; Dispersion theory.		
20. ABSTRACT (Continue on reverse side if necessary and identify by block number) This report concerns the development of methods for obtaining the optical constants of anisotropic crystals of the triclinic and monoclinic systems. The principal method used, classical dispersion theory, is adapted to these crystal systems by extending the Lorentz line parameters to include the angles characterizing the individual resonances, and by replacing the dielectric constant by a dielectric tensor. The sample crystals are gypsum, orthoclase and chalcantite. The derived optical constants are shown to be suitable for		

20. Abstract

modeling the optical properties of particulate media in the infrared spectral region. For those materials where suitable size single crystals are not available, an extension of a previously used method is applied to alabaster, a polycrystalline material of the monoclinic crystal system. *Keywords:*

Top A

Accession for	
NTIS GRA&I	<input checked="" type="checkbox"/>
DTIC TAB	<input type="checkbox"/>
Unannounced	<input type="checkbox"/>
Justification	
Distribution/	
Availability Codes	
Dist	Avail and/or Special
A-1	



TABLE OF CONTENTS

	<u>Page</u>
LIST OF TABLES	iv.
LIST OF FIGURES	v.
I. INTRODUCTION	1
II. NUMERICAL METHOD FOR TRICLINIC CRYSTALS	6
A. PREFACE	6
B. DIELECTRIC TENSOR OF TRICLINIC CRYSTALS	6
1. DISCUSSION OF EIGENVALUE PROBLEM	6
2. CALCULATION OF DIELECTRIC TENSOR FROM LORENTZ LINE PARAMETERS	13
III. SIMULATIONS OF POWDER SPECTRA USING DERIVED OPTICAL CONSTANTS	19
IV. SUMMARY	26
V. REFERENCES	27-28

LIST OF TABLES

Table No.

Page

1. Lorentz Line Parameters for Alabaster, Range of
Validity $450\text{ cm}^{-1} < \nu < 1500\text{ cm}^{-1}$

24

LIST OF FIGURES

<u>Figure No.</u>		<u>Page</u>
1.	Emittance Spectrum of Chalcantite	20
2.	Emittance Spectrum of Enstatite	21
3.	Reflectance Spectrum of Alabaster Fitted With 5 Lorentz Lines	23
4.	Emittance Spectrum of Gypsum	25

INTRODUCTION

Computer modeling of the optical properties of particulate materials is a valuable technique that is useful in research concerning atmospheric aerosols either natural or man-made (smoke screens). It is also important in development of camouflage paints or coatings and has uses in the description of the optical and thermal properties of materials which are important in such areas as insulation, solar collection, remote sensing and related topics. Such computer simulations have been seriously hampered by lack of the optical constants (the real and imaginary parts of the complex refractive index), particularly in the infrared spectral region, for many materials that may prove to be of technical significance.

A considerable body of recent research has gone into the development of methods for extracting the optical constants of solids^{1,2,3}. At the time of the inception of this work the status of the problem was that isotropic materials such as amorphous solids and cubic crystals were well described by a complex refractive index which varies with the frequency of the radiation. That refractive index could be obtained by well known techniques involving the measurement of the reflectance spectrum of such materials either at two angles⁴ two polarizations,⁵ or a combination of transmittance and reflectance⁶. It would normally be thought that in order to obtain the values of two quantities such as n , the real and k , the imaginary part of the complex refractive index, m at any frequency two measurements would be needed as just discussed. However, use of a single measurement (at each frequency) has been employed with considerable success in recent years (i.e. using classical dispersion theory)⁷. In brief, by invoking an assumed spectral line shape (the Lorentz shape) one can make a single measurement

of reflectance or of transmittance over a considerable spectral band and fit the data to a set of dispersion parameters (Lorentz line parameters) either using a reflection or transmission method.

Another method has had much usage over the years, i.e., Kramers Kronig^{8,9} analysis. This method involves a relationship between n and k , but requires that the spectrum be measured over all frequencies or that an adequate estimate be made of the high and low frequency values. These values at wavelengths or frequencies inaccessible to measurement must be known in order that the values within the spectral range of interest be not distorted. This is not true of the classical dispersion parameter method, as it has been shown¹⁰ that regardless of the values outside the range of interest, if the reflection bands are well fit within a given spectral range, the optical constants obtained are appropriate for that range.

Another advantage of the classical dispersion theory approach to extraction of optical constants is the convenience for computations of storing the information in a small file of $3N + 1$ parameters where N is the required number of oscillators. Such tables of ϵ_∞ the dielectric constant at high frequency ν_k the frequency, S_k the strength and γ_k the damping for each of the independent oscillators are very small relative to the multitude of values of n and k required to make computations at a large number of spectral frequencies.

The optical constants are calculated as needed at any frequency by the use

of the Lorentz formula $m^2 = \epsilon = \epsilon_\infty + \sum_{k=1}^N \frac{S_k}{1 + i \gamma_k \left(\frac{\nu}{\nu_k} \right) - \left(\frac{\nu}{\nu_k} \right)^2}$

where ϵ is the complex dielectric constant. Typically, somewhat less than 20 lines, occasionally as few as 1 or 2 can be used to represent the entire spectrum throughout the infrared region.

It has been shown that in cases where the absorption coefficient is large the reflection method works quite well^{2,11} and in cases where the absorption coefficient is small compared to the refractive index (organics) a transmission method using a Brewster angle of incidence is appropriate¹².

The optical constants so derived have been used together with our theoretical methods to predict or simulate the spectra of particulate materials¹³, lunar soils¹⁴, paints¹² and aerosols¹⁵.

Extensions of these methods to uniaxial symmetry crystals have been carried out⁷ and in practice turn out to be straightforward. Such crystals are treated as if they were, in fact, composed of two independent materials; one corresponding to the ordinary ray, one corresponding to the extraordinary ray. These separate refractive indices are used to make suitable calculations of cross sections for the materials involved and then combined in a 2 to 1 ratio ($E_{\perp c} : E_{\parallel c}$)^{16, 17} assuming that the particles are randomly distributed in orientation. c refers to the crystallographic high symmetry axis. This technique has proven to result in simulated spectra very closely approximating the measured spectra. The natural extension of this method to biaxial crystals is obvious for those of the orthorhombic system. Using a polarizer and appropriate crystal orientations one may extract three sets of optical constants¹¹ and when theoretical computations for powders or aerosols are made these are used in ratio of 1 to 1 to 1 for ($E_{\parallel a}$, $E_{\parallel b}$ and $E_{\parallel c}$) again assuming no preferred orientation.

The present report details how the methods for obtaining the optical constants have been extended to the low symmetry monoclinic and triclinic crystal systems. We were aided in developing our methodology by finding two papers dealing with the monoclinic problem^{18,19}. These papers suggested a method of carrying out a dispersion theory analysis for monoclinic crystals using measurements obtained from the a-c crystallographic plane. We studied the work of these authors and combined their approach with the approach that we have already taken with respect to the simpler crystal systems². The results of this work applied to gypsum were published in Ref. 20. In that paper we not only derived the optical constants for gypsum, but showed that these optical constants were appropriate for simulating the emittance spectra of gypsum powder using our previously developed theory. We also used the parameters developed by the Russians^{18,19,21} for spodumene and showed that, as with gypsum the optical constants are indeed suitable for modeling the emittance of powders. Further monoclinic work has recently been submitted for publication²² concerning the mineral orthoclase.

The most difficult problem, that of triclinic crystals, was attacked using the insights gained by the study of the monoclinic problem. The theoretical paper concerning the method of carrying out the analysis was, in fact, the first one published²³ during the work on this contract. A reduction of that method to practice was later published using Chalcantite ($\text{CuSO}_4 \cdot 5 \text{H}_2\text{O}$).²⁴ Thus the body of our work on this contract has been described in four publications.

However, some of the details have not yet been published. The following section will delineate the unpublished work. That work includes study of the monoclinic substance alabaster, which is polycrystalline gypsum. It is intended as an example of the usefulness of carrying out classical dispersion analysis of materials for which sufficiently large single crystals are not available. We had previously carried out such analysis for quartzite²⁵ but needed to show that the same type of analysis could be carried out for the low symmetry crystal systems.

In addition, we show a comparison of the measured experimental emittance of chancanthite powder to the predicted spectrum using the optical constants of that triclinic crystal. This was not included in the paper on chalcantite owing to the simplicity of the spectrum, which we felt would not contribute materially to the paper.

Another biaxial crystal powder, orthorhombic enstatite was measured and its spectrum simulated using optical constants previously obtained¹¹.

Finally, the triclinic problem as discussed in Reference 27 proved quite difficult to implement in such a way that the convergence was entirely satisfactory. While the optical constants obtained proved useful and sensible we believe that the convergence could yet be improved. We therefore did not previously describe the mathematics of the computer program in detail, but feel that it should be presented here, if only to give readers a chance to improve on our algorithms.

II. Numerical Method for Triclinic Crystals

A. Preface

In the description of the numerical methods used to fit the theoretical spectra to the observed spectra, it is assumed that the reader is conversant with references 2 and 23. In the present work we follow the scheme outlined in the latter paper with certain exceptions, the principal change being that we use normalized eigenvectors in place of the eigenvectors (a_1, b_1) , (a_2, b_2) defined by Equations (43) through (46) in reference 23. We also use numerical subscripts 1,2,3 to designate x, y, z axes, respectively.

B. Dielectric Tensor of Triclinic Crystals

1. Discussion of Eigenvalue Problem

In order to apply our usual method to find the Lorentz line parameters we must calculate the derivatives of $|r_{11}|^2 + |r_{12}|^2$ and hence r_{11} and r_{12} with respect to all the parameters. As an instructive preliminary, however, we shall study the unusual eigenvalue problem.

$$\epsilon x_j = p_j \zeta_j, \quad j = 1, 2 \quad (1)$$

which plays a central role in the derivation of the reflectance of triclinic crystals. In equation (1) we have set

$$\epsilon = \begin{pmatrix} \epsilon_{11} & \epsilon_{12} & \epsilon_{13} \\ \epsilon_{12} & \epsilon_{22} & \epsilon_{23} \\ \epsilon_{13} & \epsilon_{23} & \epsilon_{33} \end{pmatrix}, \text{ the dielectric tensor} \quad (2)$$

$$x_j = \begin{pmatrix} x_{1j} \\ x_{2j} \\ x_{3j} \end{pmatrix}, \text{ the augmented eigenvector} \quad (3)$$

$$\zeta_j = \begin{pmatrix} x_{1j} \\ x_{2j} \\ 0 \end{pmatrix}, \text{ the eigenvector} \quad (4)$$

and p_j is the eigenvalue, which may be found by solution of the quadratic equation

$$\begin{vmatrix} \epsilon_{11} - p_j & \epsilon_{12} & \epsilon_{13} \\ \epsilon_{12} & \epsilon_{22} - p_j & \epsilon_{23} \\ \epsilon_{13} & \epsilon_{23} & \epsilon_{33} \end{vmatrix} = 0 \quad (5)$$

We normalize the eigenvector x_j so that

$$x_{1j}^2 + x_{2j}^2 = 1 \quad (6)$$

$$\text{Let } a_j = \epsilon_{12} \epsilon_{23} - \epsilon_{13} (\epsilon_{22} - p_j) \quad (7)$$

$$b_j = \epsilon_{12} \epsilon_{13} - \epsilon_{23} (\epsilon_{11} - p_j) \quad (8)$$

$$c_j = (\epsilon_{11} - p_j) (\epsilon_{22} - p_j) - \epsilon_{12}^2 \quad (9)$$

$$\text{Then } x_{1j} = \frac{a_j}{(a_j^2 + b_j^2)^{1/2}} \quad (10)$$

$$x_{2j} = \frac{b_j}{(a_j^2 + b_j^2)^{1/2}} \quad (11)$$

$$x_{3j} = \frac{c_j}{(a_j^2 + b_j^2)^{1/2}} \quad (12)$$

On account of the symmetry of ϵ , the vectors ξ_1 & ξ_2 are orthogonal. We take the sign

of the second eigenvector so that

$$x_{11} = x_{22} , \quad x_{12} = -x_{21} \quad (13),(14)$$

This choice of sign convention is arbitrary, but it is imperative to stick to one convention. Ours makes the determinant

$$\begin{vmatrix} x_{11} & x_{12} \\ x_{21} & x_{22} \end{vmatrix} = 1 \quad (15)$$

instead of -1 .

In terms of the components of the normalized eigenvectors we find the amplitude reflectances to be

$$r_{11} = 2 \left(\frac{x_{11}^2}{1+q_1} + \frac{x_{12}^2}{1+q_2} \right) - 1 \quad (16)$$

$$r_{12} = 2 x_{11} x_{12} \left(\frac{1}{1+q_1} - \frac{1}{1+q_2} \right) \quad (17)$$

$$\text{where } q_j = p_j^{1/2} \quad [\text{Re}(q_j) > 0] \quad (18)$$

Before we leave the eigenvector problem, we calculate derivatives of the eigenvalues and augmented eigenvector x_j with respect to the elements of ϵ in anticipation of our later need for them.

To start, take the differential of Eq. (1)

$$\epsilon dx + d\epsilon x = dp\zeta + p d\zeta \quad (19)$$

The subscript j has been omitted, but remains understood. Multiply by ζ^T (the superscript T stands for "transpose")

$$\zeta^T \epsilon dx + \zeta^T d\epsilon x = dp \zeta^T \zeta + p \zeta^T d\zeta \quad (20)$$

Note $\zeta^T \zeta = 1$ and $(\zeta^T + d\zeta^T)(\zeta + d\zeta) = 1$ so

$$\zeta^T d\zeta = 0 \quad (21)$$

Thus we have

$$\zeta^T \epsilon dx + \zeta^T d\epsilon x = dp \quad (22)$$

Since

$$x = \zeta + \begin{pmatrix} 0 \\ 0 \\ x_3 \end{pmatrix} \quad (23)$$

it follows that

$$\epsilon \zeta = \epsilon x - \epsilon \begin{pmatrix} 0 \\ 0 \\ x_3 \end{pmatrix} \quad (24)$$

or

$$\epsilon \zeta = p \zeta - \begin{pmatrix} \epsilon_{13} \\ \epsilon_{23} \\ \epsilon_{33} \end{pmatrix} x_3 \quad (25)$$

Therefore

$$\zeta^T \epsilon dx = dx^T \epsilon \zeta = p dx^T \zeta - dx^T \begin{pmatrix} \epsilon_{13} \\ \epsilon_{23} \\ \epsilon_{33} \end{pmatrix} x_3 \quad (26)$$

But

$$dx^T \zeta = 0 \quad (27)$$

so

$$\zeta^T \epsilon dx = -x_3 (\epsilon_{13} dx_1 + \epsilon_{23} dx_2 + \epsilon_{33} dx_3) \quad (28)$$

Because the third element of ζ is zero we see that

$$\epsilon_{13} x_1 + \epsilon_{23} x_2 + \epsilon_{33} x_3 = 0 \quad (29)$$

$$\text{and, therefore, } \epsilon_{13} dx_1 + \epsilon_{23} dx_2 + \epsilon_{33} dx_3 = -x_1 d\epsilon_{13} - x_2 d\epsilon_{23} - x_3 d\epsilon_{33} \quad (30)$$

$$\text{so } \zeta^T dx = x_1 x_3 d\epsilon_{13} + x_2 x_3 d\epsilon_{23} + x_3^2 d\epsilon_{33} \quad (31)$$

Substitute this result into Eq. (22) to find

$$dp = \zeta^T dx + x_1 x_3 d\epsilon_{13} + x_2 x_3 d\epsilon_{23} + x_3^2 d\epsilon_{33} \quad (32)$$

Now all we have to do is to let one $d\epsilon_{\alpha\beta}$ be non-zero at a time to find the partial derivative of p with respect to the element of the dielectric tensor $\epsilon_{\alpha\beta}$. The results may be summarized very simply.

$$\frac{\partial p_j}{\partial \epsilon_{\alpha\alpha}} = x_{\alpha j}^2; \quad \frac{\partial p_j}{\partial \epsilon_{\alpha\beta}} = 2x_{\alpha j} x_{\beta j} \quad (\alpha \neq \beta) \quad (33)$$

or even more succinctly

$$\frac{\partial p_j}{\partial \epsilon_{\alpha\beta}} = (2 - \delta_{\alpha\beta}) x_{\alpha j} x_{\beta j} \quad (34)$$

where $\delta_{\alpha\beta}$ is the Kronecker symbol (unity when $\alpha = \beta$, zero otherwise)

We still must calculate the derivatives of x_{11} , x_{21} and x_{31} with respect to the elements $\epsilon_{\alpha\beta}$. We cannot solve Eq. (19) for dx_{11} , dx_{21} , dx_{31} because the matrix of the coefficients of these differentials is singular [Eq. (5)], but Eq. (21) supplies an independent condition. Since ζ_1 and ζ_2 are orthogonal, it follows that dx_{11} and dx_{21} are proportional to x_{12} and x_{22} , respectively. In fact we may write

$$dx_{11} = A_{\alpha\beta} x_{12} d\epsilon_{\alpha\beta}, \quad dx_{21} = A_{\alpha\beta} x_{22} d\epsilon_{\alpha\beta}, \quad dx_{31} = (A_{\alpha\beta} x_{32} + B_{\alpha\beta}) d\epsilon_{\alpha\beta} \quad (35)$$

We also find, when we assume only one $d\epsilon_{\alpha\beta} \neq 0$, that we can write

$$d\epsilon x_1 = \begin{pmatrix} u_1 \\ u_2 \\ u_3 \end{pmatrix} d\epsilon_{\alpha\beta} \quad (36)$$

with $u_\alpha = x_{\alpha 1}$ for $\alpha = \beta$
 $u_\alpha = x_{\beta 1}$, $u_\beta = x_{\alpha 1}$ for $\alpha \neq \beta$
the otherwise undefined components of u being zero.

Now substitute Equations (35) and (36) into Equation (19) and divide by $d\epsilon_{\alpha\beta}$. In expanded form we see that

$$\left\{ \begin{pmatrix} \epsilon_{11} & \epsilon_{12} & \epsilon_{13} \\ \epsilon_{12} & \epsilon_{22} & \epsilon_{23} \\ \epsilon_{13} & \epsilon_{23} & \epsilon_{33} \end{pmatrix} - \begin{pmatrix} p_1 & 0 & 0 \\ 0 & p_1 & 0 \\ 0 & 0 & 0 \end{pmatrix} \right\} \left\{ A_{\alpha\beta} \begin{pmatrix} x_{12} \\ x_{22} \\ x_{32} \end{pmatrix} + \begin{pmatrix} 0 \\ 0 \\ B_{\alpha\beta} \end{pmatrix} \right\} \\ = \frac{\partial p_1}{\partial \epsilon_{\alpha\beta}} \begin{pmatrix} x_{11} \\ x_{21} \\ 0 \end{pmatrix} - \begin{pmatrix} u_1 \\ u_2 \\ u_3 \end{pmatrix} \quad (37)$$

Since $\epsilon x_2 = p_2 \zeta_2$, the first two rows of (37) are seen to yield the two equations for $A_{\alpha\beta}$ and $B_{\alpha\beta}$

$$\left. \begin{aligned} (p_2 - p_1) x_{12} A_{\alpha\beta} + \epsilon_{13} B_{\alpha\beta} &= x_{11} \frac{\partial p_1}{\partial \epsilon_{\alpha\beta}} - u_1 \\ (p_2 - p_1) x_{22} A_{\alpha\beta} + \epsilon_{23} B_{\alpha\beta} &= x_{21} \frac{\partial p_1}{\partial \epsilon_{\alpha\beta}} - u_2 \end{aligned} \right\} \quad (38)$$

Equation (38) can be solved by Cramer's rule. For the determinant Δ we find

$$\Delta = (p_2 - p_1) \epsilon_{33} x_{31} \quad (39)$$

$$\text{since } \epsilon_{23} x_{12} - \epsilon_{13} x_{22} = -\epsilon_{23} x_{21} - \epsilon_{13} x_{11} = \epsilon_{33} x_{31} \quad (40)$$

$$\text{hence } A_{\alpha\beta} = \frac{(\epsilon_{23} x_{11} - \epsilon_{13} x_{21}) \frac{\partial p_1}{\partial \epsilon_{\alpha\beta}} - \epsilon_{23} u_1 + \epsilon_{13} u_2}{(p_2 - p_1) \epsilon_{33} x_{31}} \quad (41)$$

$$B_{\alpha\beta} = \frac{x_{11} u_1 + x_{21} u_2 - \frac{\partial p_1}{\partial \epsilon_{\alpha\beta}}}{\epsilon_{33} x_{31}} \quad (42)$$

All that remains is to evaluate these expressions for pairs α & β to find

$$\left. \begin{aligned}
 A_{11} &= \frac{x_{11} x_{21}}{p_2 - p_1} & B_{11} &= 0 \\
 A_{12} &= \frac{x_{21}^2 - x_{11}^2}{p_2 - p_1} & B_{12} &= 0 \\
 A_{13} &= -\frac{1}{\epsilon_{33}} (2\epsilon_{13} A_{11} + \epsilon_{23} A_{12}) & B_{13} &= -\frac{x_{11}}{\epsilon_{33}} \\
 A_{22} &= -\frac{x_{11} x_{21}}{p_2 - p_1} = -A_{11} & B_{22} &= 0 \\
 A_{23} &= -\frac{1}{\epsilon_{33}} (2\epsilon_{23} A_{22} + \epsilon_{13} A_{12}) & B_{23} &= -\frac{x_{21}}{\epsilon_{33}} \\
 A_{33} &= -\frac{x_{31} x_{32}}{p_2 - p_1} & B_{33} &= -\frac{x_{31}}{\epsilon_{33}}
 \end{aligned} \right\} \quad (43)$$

The derivatives are calculated from the equations

$$\left. \begin{aligned}
 \frac{\partial x_{11}}{\partial \epsilon_{\alpha\beta}} &= A_{\alpha\beta} x_{12} \\
 \frac{\partial x_{21}}{\partial \epsilon_{\alpha\beta}} &= A_{\alpha\beta} x_{22} \\
 \frac{\partial x_{31}}{\partial \epsilon_{\alpha\beta}} &= A_{\alpha\beta} x_{32} + B_{\alpha\beta}
 \end{aligned} \right\} \quad (44)$$

The derivatives of x_{31} are not going to be needed later, but are included here for completeness of the exposition.

2. Calculation of Dielectric Tensor from Lorentz Line Parameters

Two sets of coordinate axes must be defined in this aspect of the problem. One is fixed in the crystal, the other is fixed in the interferometer spectrometer.

The axes of the crystal will be called x, y & z. Let the x-axis be identical with the a-axis of the crystal. Let the y-axis be in the a-b plane but perpendicular to the x-axis. The z-axis is placed perpendicular to both x-axis & y-axis to form a right handed system (xyz).

The axes in the interferometer are such that the plane of polarization of the light incident on the crystal face is along the 1-axis; the light propagates along the 3-axis. The 2-axis is chosen perpendicular to the 1- & 3-axes to form a right handed system (1, 2, 3).

To model the experiment on the crystal, the crystal properties, expressed in the (x, y, z) axes must be rotated into the (1, 2, 3) system. To do this we must set up a rotation matrix S (R is reserved for reflectance) with elements S_{ij} chosen so that

$$\begin{pmatrix} S_{11} \\ S_{21} \\ S_{31} \end{pmatrix} \text{ is the unit vector } \hat{x} \text{ expressed in the interferometer or lab system} \quad (45a)$$

$$\begin{pmatrix} S_{12} \\ S_{22} \\ S_{32} \end{pmatrix} \text{ and } \begin{pmatrix} S_{13} \\ S_{23} \\ S_{33} \end{pmatrix} \text{ are the unit vectors } \hat{y} \text{ and } \hat{z} \text{ expressed similarly} \quad (45b)$$

Now suppose we know the dielectric tensor, $\tilde{\epsilon}$, referred to the crystal axes. Then the tensor in the lab system is

$$\epsilon = S \tilde{\epsilon} S^T \quad (46)$$

$$\text{and } \frac{\partial \epsilon}{\partial p_{\ell k}} = S \frac{\partial \tilde{\epsilon}}{\partial p_{\ell k}} S^T \quad (47)$$

under the assumption that the Lorentz lines occur independently of each other (instead of in orthogonal triads) we have, in the crystal system

$$\tilde{\epsilon} = \tilde{\epsilon}^{\infty} + \sum_{k=1}^K v_k v_k^T L_k \quad (48)$$

where $\tilde{\epsilon}^{\infty}$ has components ϵ_{xx}^{∞} , ϵ_{xy}^{∞} etc. & is a symmetrical tensor representing the dielectric constant at high frequencies.

$$v_k = \begin{pmatrix} \sin \theta_k \cos \Phi_k \\ \sin \theta_k \sin \Phi_k \\ \cos \theta_k \end{pmatrix}, \text{ giving the orientation of the dipole} \quad (49)$$

$$L_k = \frac{S_k}{1 + i\gamma_k \frac{\nu}{\nu_k} - \left(\frac{\nu}{\nu_k}\right)^2}, \text{ the usual resonance formula.} \quad (50)$$

We further define Lorentz line parameters p_{0k} as follows:

$$\tilde{\epsilon}^{\infty} = \begin{pmatrix} p_{01} & p_{02} & p_{03} \\ p_{02} & p_{04} & p_{05} \\ p_{03} & p_{05} & p_{06} \end{pmatrix} \quad (51)$$

$$\left. \begin{aligned} p_{1k} &= S_k \\ p_{2k} &= \gamma_k / \nu_k \\ p_{3k} &= \nu_k^{-2} \\ p_{4k} &= \theta_k \\ p_{5k} &= \Phi_k \end{aligned} \right\} \quad (52)$$

In order to perform "Newton's Descent" to calculate the best parameters to minimize the evil²⁰, we need the matrix UU^T whose elements are

$$\sum_{e=1}^E \frac{\partial R}{\partial p_{0k}} (\nu_e, p) \frac{\partial R}{\partial p_{0\lambda}} (\nu_e, p) \quad (53)$$

where E is the total number of experimental reflectance measurements made and $\ell k, \lambda k$ run over all possible values that have been defined.

As before

$$\frac{\partial R}{\partial p_{\ell k}} = 2 \operatorname{Re} \left(r_{11}^* \frac{\partial r_{11}}{\partial p_{\ell k}} + r_{12}^* \frac{\partial r_{12}}{\partial p_{\ell k}} \right) \quad (54)$$

$$\text{and } \frac{\partial r_{ij}}{\partial p_{\ell k}} = \sum_{\alpha\beta} \frac{\partial r_{ij}}{\partial \epsilon_{\alpha\beta}} \frac{\partial \epsilon_{\alpha\beta}}{\partial p_{\ell k}} \quad (6 \text{ terms : } \alpha\beta=11,12,13,22,23,33) \quad (55)$$

$$\text{Since } r_{11} = 2 \left(\frac{x_{11}^2}{1+q_1} + \frac{x_{21}^2}{1+q_2} \right) - 1 \quad (56)$$

$$\& \quad r_{12} = 2 x_{11} x_{21} \left(\frac{1}{1+q_1} - \frac{1}{1+q_2} \right) \quad (57)$$

we write

$$\frac{\partial r_{ij}}{\partial \epsilon_{\alpha\beta}} = \frac{\partial r_{ij}}{\partial x_{11}} \frac{\partial x_{11}}{\partial \epsilon_{\alpha\beta}} + \frac{\partial r_{ij}}{\partial x_{21}} \frac{\partial x_{21}}{\partial \epsilon_{\alpha\beta}} + \frac{\partial r_{ij}}{\partial q_1} \frac{\partial q_1}{\partial \epsilon_{\alpha\beta}} + \frac{\partial r_{ij}}{\partial q_2} \frac{\partial q_2}{\partial \epsilon_{\alpha\beta}} \quad (58)$$

From (56) & (57) we see

$$\frac{\partial r_{11}}{\partial x_{11}} = \frac{4 x_{11}}{1+q_1} \quad \frac{\partial r_{12}}{\partial x_{11}} = 2 x_{21} \left(\frac{1}{1+q_1} - \frac{1}{1+q_2} \right) \quad (59)$$

$$\frac{\partial r_{11}}{\partial x_{21}} = \frac{4 x_{21}}{1+q_2} \quad \frac{\partial r_{12}}{\partial x_{21}} = 2 x_{11} \left(\frac{1}{1+q_1} - \frac{1}{1+q_2} \right) \quad (60)$$

$$\frac{\partial r_{11}}{\partial q_1} = - \frac{2 x_{11}^2}{(1+q_1)^2} \quad \frac{\partial r_{12}}{\partial q_1} = - \frac{2 x_{11} x_{21}}{(1+q_1)^2} \quad (61)$$

$$\frac{\partial r_{11}}{\partial q_2} = - \frac{2 x_{21}^2}{(1 + q_2)^2} \quad \frac{\partial r_{12}}{\partial q_2} = \frac{2 x_{22} x_{21}}{(1 + q_2)^2} \quad (62)$$

We have already demonstrated that

$$\frac{\partial x_{11}}{\partial \epsilon_{\alpha\beta}} = A_{\alpha\beta} x_{12} \quad \frac{\partial x_{12}}{\partial \epsilon_{\alpha\beta}} = A_{\alpha\beta} x_{22} \quad (63)$$

and the $A_{\alpha\beta}$ have been found to be

$$A_{11} = \frac{x_{11} x_{21}}{p_2 - p_1} \quad (64)$$

$$A_{12} = \frac{x_{21}^2 - x_{11}^2}{p_2 - p_1}$$

$$\left. \begin{aligned} A_{13} &= - (2\epsilon_{13} A_{11} + \epsilon_{23} A_{12})/\epsilon_{33} \\ A_{22} &= - A_{11} \\ A_{23} &= - (2\epsilon_{23} A_{22} + \epsilon_{13} A_{12})/\epsilon_{33} \\ A_{33} &= - x_{31} x_{32}/(p_2 - p_1) \end{aligned} \right\} \quad (65)$$

Obviously, from (33), we have

$$\frac{\partial q_j}{\partial \epsilon_{\alpha\alpha}} = \frac{1}{2} x_{\alpha j}^2 / q_j \quad \frac{\partial q_j}{\partial \epsilon_{\alpha\beta}} = x_{\alpha j} x_{\beta j} / q_j \quad (66)$$

So the computation of $\frac{\partial r_{ij}}{\partial \epsilon_{\alpha\beta}}$ is defined. We must therefore calculate the derivatives

$$\frac{\partial \epsilon_{\alpha\beta}}{\partial p_{\ell k}} . \text{ For the entire matrix}$$

$$\frac{\partial \epsilon}{\partial p_{\ell k}} = S \frac{\partial \tilde{\epsilon}}{\partial p_{\ell k}} S^T \quad (67)$$

So we confine ourselves to the calculation of $\frac{\partial \tilde{\epsilon}}{\partial p_{\ell k}}$ and suppose the results will be rotated

numerically into the (1,2,3) (lab) system.

To start with,

$$\frac{\partial \tilde{\epsilon}}{\partial p_{01}} = \begin{pmatrix} 1 & 0 & 0 \\ 0 & 0 & 0 \\ 0 & 0 & 0 \end{pmatrix}, \quad \frac{\partial \tilde{\epsilon}}{\partial p_{02}} = \begin{pmatrix} 0 & 1 & 0 \\ 1 & 0 & 0 \\ 0 & 0 & 0 \end{pmatrix} \text{ etc.} \quad (68)$$

The first three derivatives of the Lorentz line part of the affair are unchanged from before:

$$\frac{\partial}{\partial p_{\ell k}} (v_k v_k^T L_k) = v_k v_k^T \frac{\partial L_k}{\partial p_{\ell k}}, \quad \ell = 1, 2, 3 \quad (69)$$

$$\frac{\partial L_k}{\partial p_{1k}} = \frac{1}{D_k}, \quad D_k = 1 + i p_{2k} \nu - p_{3k} \nu^2 \quad (70)$$

$$\frac{\partial L_k}{\partial p_{2k}} = -i \nu \frac{L_k}{D_k} \quad (71)$$

$$\frac{\partial L_k}{\partial p_{3k}} = \nu^2 \frac{L_k}{D_k} \quad (72)$$

$$\text{But } \frac{\partial}{\partial p_{\ell k}} (v_k v_k^T L_k) = \left(\frac{\partial v_k}{\partial p_{\ell k}} v_k^T + v_k \frac{\partial v_k^T}{\partial p_{\ell k}} \right) L_k, \quad \ell = 4, 5 \quad (73)$$

$$\frac{\partial v_k^T}{\partial p_{4k}} = (\cos p_{4k} \cos p_{5k}, \cos p_{4k} \sin p_{5k}, -\sin p_{4k}) \quad (74)$$

$$\frac{\partial v_k^T}{\partial p_{5k}} = (-\sin p_{4k} \sin p_{5k}, \sin p_{4k} \cos p_{5k}, 0) \quad (75)$$

$$\text{Obviously } \frac{\partial v_k}{\partial p_{\ell k}} v_k^T = \left(v_k \frac{\partial v_k^T}{\partial p_{\ell k}} \right)^T \quad (76)$$

A Fortran program embodying these methods was written and used to fit the observed spectra. Convergence, however was not satisfactory for reasons that are still unknown.

All of the algebra and the coding was checked by independent computation. To perform the checking, a program was written for a HP41CX to calculate the reflectance R as a function of the Lorentz line parameters. Derivatives were checked by comparing values obtained by the Fortran program with those obtained from the HP41CX by numerical differentiation.

III. Simulations of Powder Spectra using Derived Optical Constants

As mentioned above, the usefulness of our derived optical constants can be evaluated by examining the spectra simulated with them in comparison to measured emittance spectra of powders. Such comparisons were carried out in References 20 and 22 during the contract. Figure 1 shows such a comparison for chalcantite powder. This comparison shows good agreement between the experimental data and the simulated spectrum using the three sets of optical constants derived in Reference 24. The spectrum is, however, so simple that we did not believe it provided a convincing proof of the validity of our method.

A better case is shown for enstatite in Figure 2. The three sets of optical constants for this material had been derived previously by classical dispersion theory¹¹. As enstatite is orthorhombic it was used as a test of our use of a 1:1:1 ratio of the three sets of optical constants for randomly oriented biaxial powders where the crystal axes are orthogonal.

Finally, there remains the problem of obtaining useful optical constants for modeling purposes with those crystals for which a sufficiently large single crystal cannot be obtained. The method we have chosen to attempt for such materials consists of measuring the reflectance spectrum of a polycrystalline sample and obtaining optical constants as if this material was isotropic. The resulting values are clearly, not rigorous, representing the surface (Fresnel) averaged spectrum, as this average is different from the average (cross sections) that would be appropriate for modeling of particulate materials. Nonetheless, this idea has been explored and found useful in the past.^{2,25}

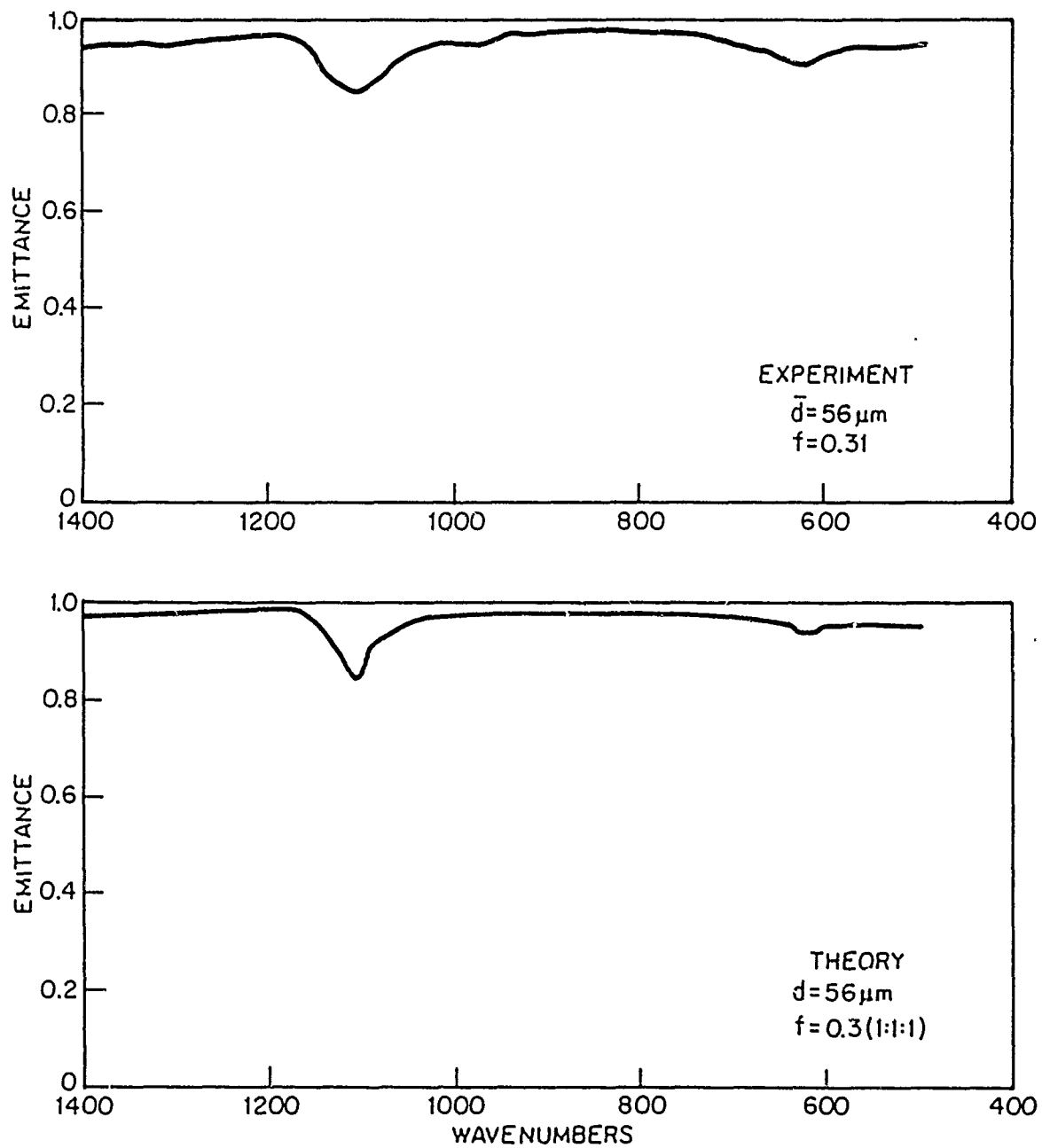


FIGURE 1 EMITTANCE SPECTRUM OF CHALCANTHITE

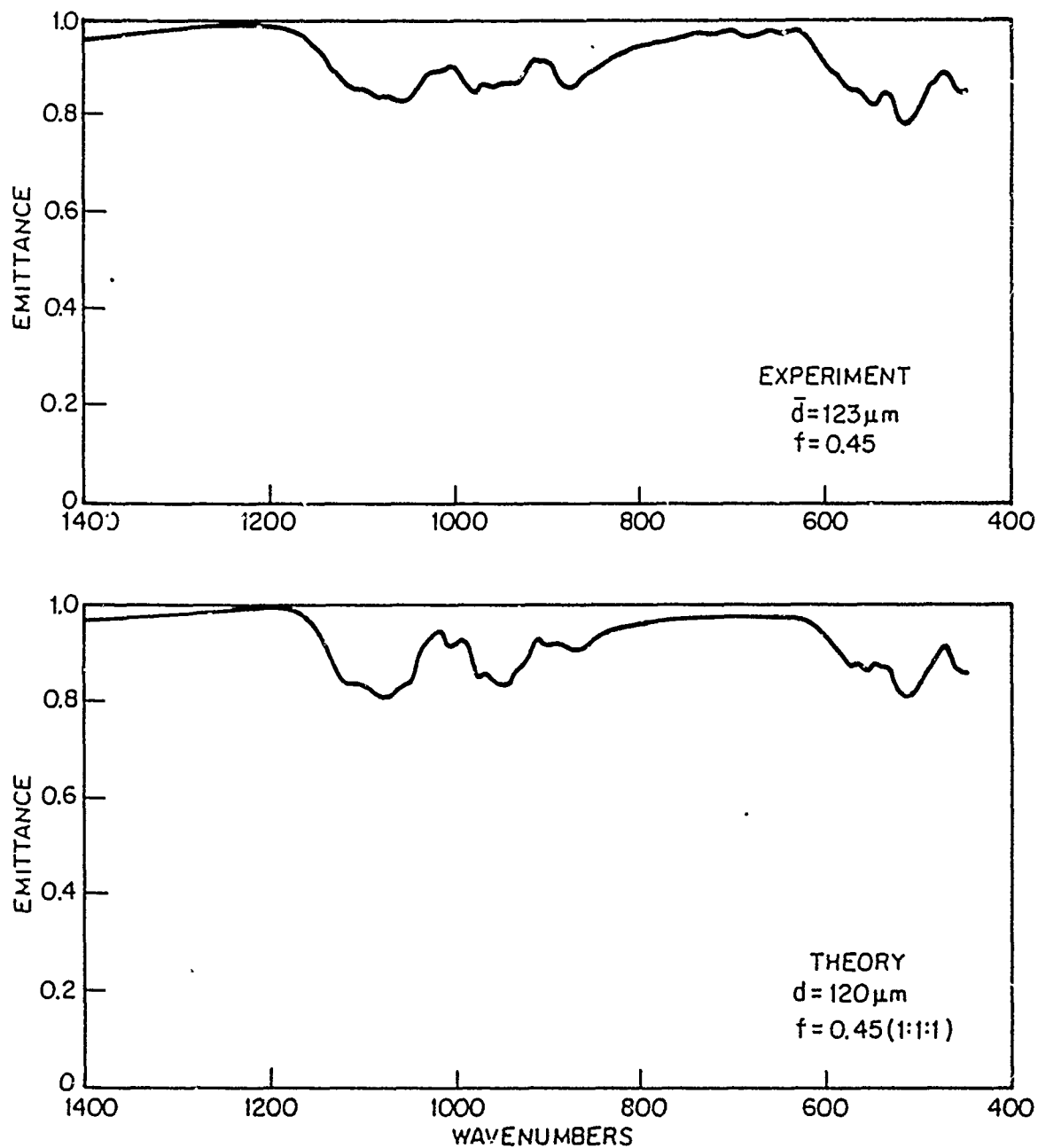


FIGURE 2 EMITTANCE SPECTRUM OF ENSTATITE

In order to carry out the same kind of test of "pseudo" optical constants for a low symmetry crystal we chose to use alabaster which is a polycrystalline form of gypsum.

A sample obtained from Wards Natural Science Establishment was cut and polished and its reflectance spectrum obtained using our Digilab FTS 15C Interferometer Spectrometer with the Harrick NIRA²⁰ attachment. Rapid convergence to the Lorentz line parameters was obtained. The values for alabaster are given in Table 1. The resulting fit is shown in Figure 3.

In Figure 4 we show the simulated spectra of the gypsum powder of Reference 20 using both the true optical constants derived from single crystal gypsum and "pseudo" optical constants obtained from alabaster. We have used an option in our powder theory program that allows for the contributions of asperities on the gypsum particles here which results in a slightly different intensity than shown in the theoretical spectrum of Reference 20. As is evident the pseudo optical constants do not give as good a fit to powder data as the true optical constants. The nature of that defect is principally that the simulated emittance features are much weaker than those observed. This is a similar result to that obtained in our previous quartzite experiment but more striking. We believe the discrepancy to result from the difficulty of obtaining a suitably high reflectance on alabaster which is hard to polish well owing to its soft character. A further discrepancy is the relative large size of the feature near 600 cm^{-1} compared with either the experiment with gypsum powder or the simulation with the true optical constants.

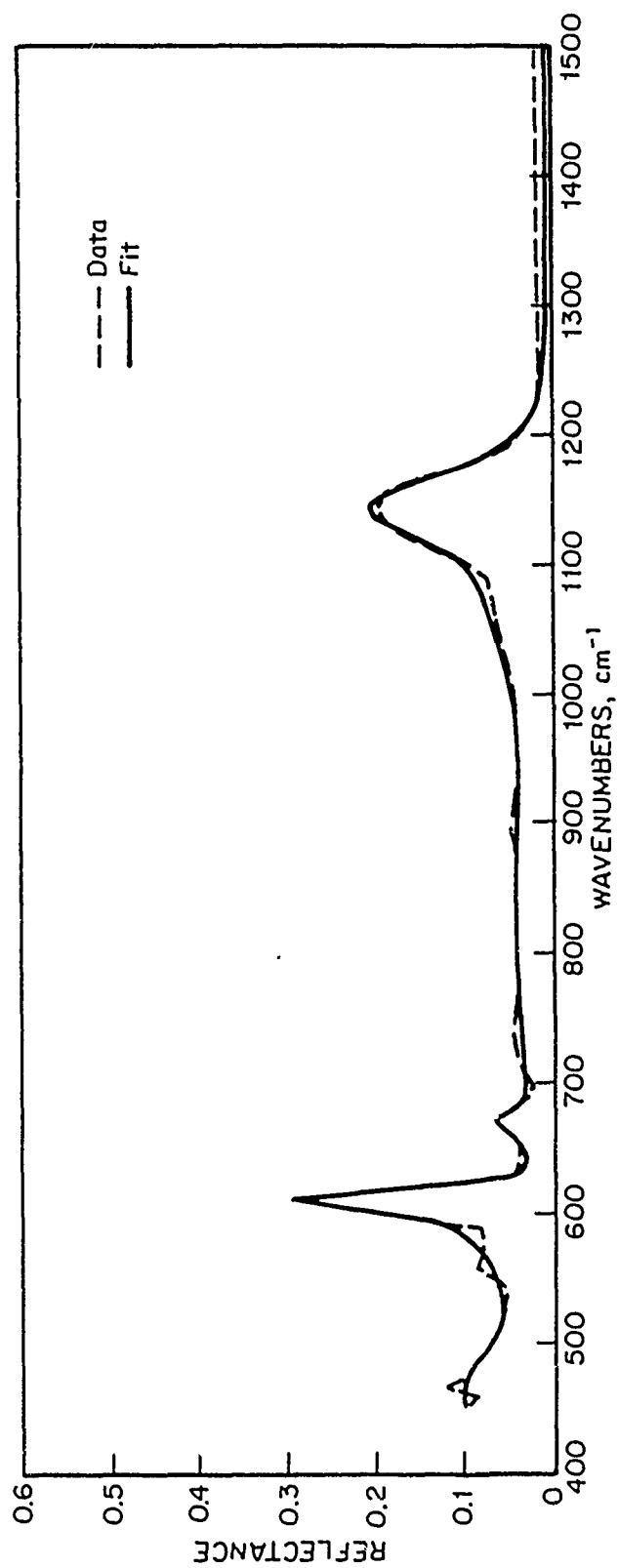


FIGURE 3 REFLECTANCE SPECTRUM OF ALABASTER FITTED WITH 5 LORENTZ LINES

k	$\nu_k (\text{cm}^{-1})$	$\sigma(\nu_k) (\text{cm}^{-1})$	S_k	$\sigma(S_k)$	γ_k	$\sigma(\gamma_k)$
1	1133.49	2.04	0.11901	0.00759	0.04031	0.00239
2	916.21	48.13	0.46825	0.09085	0.75297	0.20780
3	674.92	2.13	0.02030	0.00636	0.02392	0.00778
4	609.09	0.44	0.10420	0.00523	0.01896	0.00119
5	479.10	5.48	0.15993	0.05031	0.12694	0.03792

$$\epsilon_{\infty} = 1.7918 \quad \sigma(\epsilon_{\infty}) = .0579$$

Table 1

Lorentz Line Parameters for Alabaster, Range of Validity $450 \text{ cm}^{-1} < \nu < 1500 \text{ cm}^{-1}$

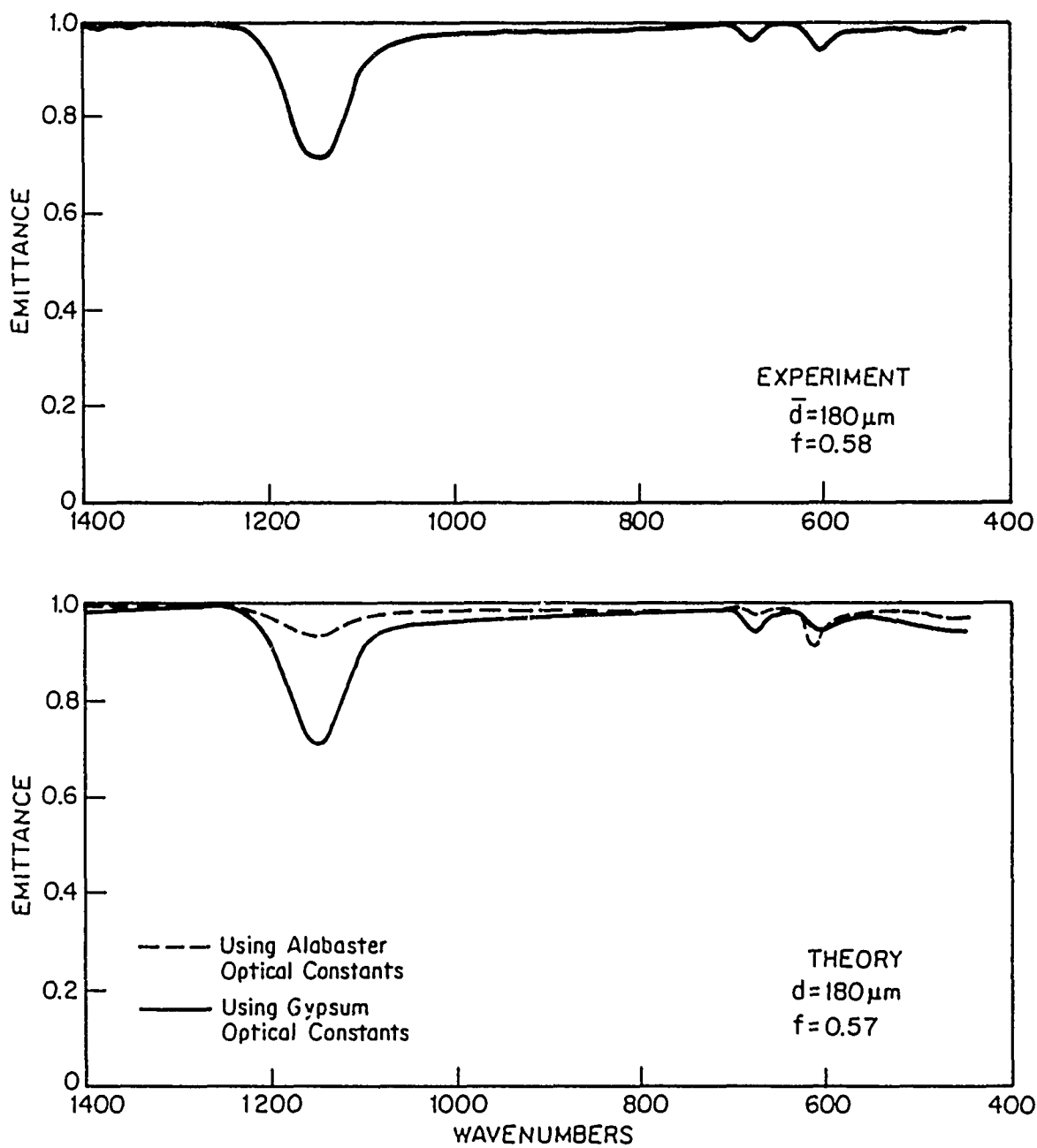


FIGURE 4 EMITTANCE SPECTRUM OF GYPSUM

IV. Summary

Methods for derivation of the optical constants of materials belonging to the triclinic and monoclinic crystal systems have been developed. These optical constants were shown to be useful in modeling the emittance spectra of powders in the infrared region. The rigorous method, which can only be used for single crystals, provides better results than an approximate method which must be used if sufficiently large single crystals are not available.

The bulk of this work has been published or submitted for publication in four papers. They are:

1. A. G. Emslie and J. R. Aronson, Determination of the Complex Dielectric Tensor of Triclinic Crystals: Theory, J. Opt. Soc. Am. 73, 916 (1983)
2. James R. Aronson, Alfred G. Emslie, Ellen V. Miseo, Emmett M. Smith and Peter F. Strong, Optical Constants of Monoclinic Anisotropic Crystals: Gypsum, Appl Opt. 22, 4093 (1983)
3. James R. Aronson, Alfred G. Emslie and Peter F. Strong, Optical Constants of Triclinic Anisotropic Crystals: Blue Vitriol, Appl. Opt. 24, 1200 (1985)
4. James R. Aronson, Optical Constants of Monoclinic Anisotropic Crystals: Orthoclase, submitted to Spectrochimica Acta (1985)

V. References

1. R. M. Roessler, Brit J. Appl. Phys. 16, 1359 (1965)
2. J. R. Aronson and P. F. Strong, Appl. Opt. 14, 2914 (1975)
3. J. W. Schaaf and D. Williams, J. Opt. Soc. Am. 63, 726 (1973)
4. I. Simon, J. Opt. Soc. Am. 41, 336 (1951)
5. C. Boeckner, J. Opt. Soc. Am. 19, 7 (1925)
6. A. Kahan, Appl. Opt. 3, 314 (1964)
7. W. G. Spitzer and D. A. Kleinman, Phys. Rev. 121, 1324 (1961)
8. R. de L. Kronig, J. Opt. Soc. Am. and Rev. Sci. Inst. 12, 547 (1926)
9. T. S. Robinson, Proc. Phys. Soc. B 65, 910 (1952)
10. H. W. Verleur, J. Opt. Soc. Am. 58, 1356 (1968)
11. J. R. Aronson, A. G. Emslie, E. M. Smith and P. F. Strong, Proc. Lunar Planet, Sci. Conf. 10th, 1787 (1979)
12. J. R. Aronson and A. G. Emslie, Final Report to U.S. Army Mobility Equipment Research and Development Command, "Modeling the Infrared Emittance of Paints", Oct. 1980 Contract #DAAK-70-79-D-0036
13. J. R. Aronson and A. G. Emslie, in Infrared and Raman Spectroscopy of Lunar and Terrestrial Minerals, C. Karr, Jr., Ed. (Academic Press, New York, 1975)
14. J. R. Aronson and E. M. Smith, Proc. Lunar Planet. Sci. Conf. 9th, 2911 (1978)
15. J. R. Aronson and A. G. Emslie, J. Geophys. Res. 80, 4925 (1975)
16. A. G. Emslie and J. R. Aronson, Appl. Opt. 12, 2563 (1973)
17. J. T. Peterson and J. A. Weinman, J. Geophys. Res. 74, 6947 (1969)
18. M. B. Belousov and V. G. Pavinich, Opt. Spektrosk. 45, 920 (1978) [Opt. Spectrosc. 45, 771 (1978)]
19. V. F. Pavinich and M. V. Belousov, Opt. Spektrosk 45, 1114 (1978) [Opt. Spectrosc. 45, 881 (1978)]
20. J. R. Aronson, A. G. Emslie, E. V. Miseo, E. M. Smith and P. F. Strong, Appl. Opt. 22, 4093 (1983)
21. A. N. Lazarev, N. O. Zulumyan, V. F. Pavinich, B. Piriou and A. P. Mirgorodskiy, Kolebaniya Okisnykh Reshetok (Nauka Publ., Leningrad 1980)

V. References (continued)

22. J. R. Aronson, submitted to Spectrochim. Acta (1985)
23. A. G. Emslie and J. R. Aronson, J. Opt. Soc. Am. 73, 916 (1983)
24. J. R. Aronson, A. G. Emslie and P. F. Strong, Appl. Opt. 24, 1200 (1985)
25. J. R. Aronson and A. G. Emslie, Appl. Opt. 19, 4128 (1980)